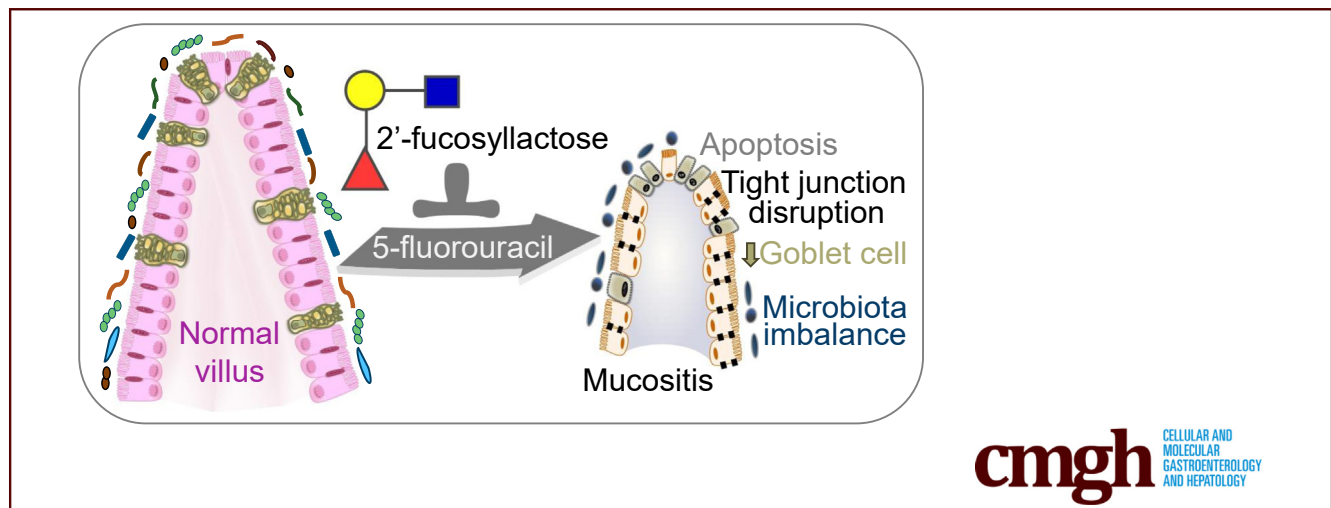


ORIGINAL RESEARCH

2'-Fucosyllactose Ameliorates Chemotherapy-Induced Intestinal Mucositis by Protecting Intestinal Epithelial Cells Against Apoptosis

Gang Zhao,¹ Jessica Williams,¹ M. Kay Washington,² Yaohua Yang,³ Jirong Long,³ Steven D. Townsend,⁴ and Fang Yan^{1,5}¹Department of Pediatrics, ²Department of Pathology, Microbiology and Immunology, ³Department of Medicine, Vanderbilt Epidemiology Center, Vanderbilt-Ingram Cancer Center, Vanderbilt University Medical Center, Nashville, Tennessee;⁴Department of Chemistry, ⁵Department of Cell and Developmental Biology, Vanderbilt University, Nashville, Tennesseecmgh CELLULAR AND
MOLECULAR
GASTROENTEROLOGY
AND HEPATOLOGY

SUMMARY

This study shows a novel direct effect of 2'-fucosyllactose, an abundant oligosaccharide in human milk, in mitigating apoptosis stimulated by the chemotherapeutic agent 5-fluorouracil in intestinal epithelial cells. The results indicated that 2'-fucosyllactose ameliorates 5-fluorouracil-induced intestinal mucositis by supporting intestinal integrity for protection against injury.

BACKGROUND & AIMS: Intestinal mucositis, a severe complication of antineoplastic therapeutics, is characterized by mucosal injury and inflammation in the small intestine. Therapies for the prevention and treatment of this disease are needed. We investigated whether 2'-fucosyllactose (2'-FL), an abundant oligosaccharide in human milk, protects intestinal integrity and ameliorates intestinal mucositis.

METHODS: A mouse small intestinal epithelial (MSIE) cell line, mouse enteroid cultures, and human gastrointestinal tumor cell lines (AGS and HT29) were co-treated with the chemotherapy agent 5-fluorouracil (5-FU) and 2'-FL. Mice were injected intraperitoneally with 5-FU to induce intestinal mucositis. 2'-FL was administered in the drinking water to mice before

(pretreatment) or concurrently with 5-FU injection. Body weight and pathologic changes were analyzed.

RESULTS: 2'-FL alleviated 5-FU inhibition of cell growth in MSIE cells, but not in AGS and HT29 cells. The 5-FU-induced apoptosis in MSIE cells and enteroids was suppressed by 2'-FL. Compared with 5-FU treatment alone, 2'-FL pretreatment protected against body weight loss, and ameliorated inflammation scores, proinflammatory cytokine production, shortening of villi, epithelial cell apoptosis, goblet cell loss, and tight junctional complex disruption in the small intestine. 2'-FL concurrent treatment had less of an effect on intestinal mucositis than 2'-FL pretreatment. Interestingly, no effect of 2'-FL was observed on 5-FU-induced S-phase arrest in MSIE, AGS, and HT29 cells. Neither pretreatment nor concurrent treatment with 2'-FL affected 5-FU-induced inhibition of proliferation in MSIE cells.

CONCLUSIONS: This study shows a novel direct effect of 2'-FL in protecting small intestinal epithelial cells against apoptosis stimulated by 5-FU, which may contribute to prevention of 5-FU-induced intestinal mucositis. (*Cell Mol Gastroenterol Hepatol* 2022;13:441–457; <https://doi.org/10.1016/j.jcmgh.2021.09.015>)

Keywords: 5-Fluorouracil; Human Milk Oligosaccharides; Intestinal Inflammation; Proliferation.

Human milk contains essential nutrients, including proteins, fatty acids, carbohydrates, and a variety of bioactive components that promote growth¹ and prevent diseases in early life, and enable long-term health benefits.² Human milk oligosaccharides (HMOs), a mixture of non-digestible carbohydrates with diverse structures, are the third most abundant solid component in human milk.³ HMOs are produced through 3 steps in the mammary glands: synthesis of lactose via β -linkage of β -D-galactose and β -D-glucose; subsequent functionalization of lactose to produce linear or branched HMOs by using N-acetyllactosamine as an elongation residue or lacto-N-biose as a terminating residue; and fucosylation or sialylation of these core oligosaccharides.^{4,5} Fucosylation requires α -2-fucosyltransferase and α 3/4-fucosyltransferase, which are present in the secretor and the Lewis blood group, respectively.⁶ The enzymes performing sialylation are unclear.⁷ Studies have shown that HMOs promote immune system development, such as tolerance and protective immunity,^{8,9} and function as prebiotics that promote the growth of beneficial gut microbiota, such as bifidobacteria and lactobacilli, in infancy; these bacteria have the enzymatic machinery to digest HMOs extracellularly or intracellularly for use as a carbon source.^{10,11} In addition, HMOs compete with pathologic bacteria and viruses for adhesion to human cells, thus exerting antibacterial activities against infectious diseases.^{10,12}

Identifying the activities of individual oligosaccharides is necessary for understanding the mechanisms involved in the action of HMOs. The compound 2'-fucosyllactose (2'-FL), an abundant component of HMOs, particularly in early lactation,¹³ is correlated with child growth during the first 5 years of life.¹⁴ Interestingly, the roles of 2'-FL in maintaining microbiome homeostasis have been found not only in early life¹⁵ but also in adulthood in human beings.¹⁶ Animal studies have further shown the anti-inflammatory effects of 2'-FL, such as decreasing colitis in mice with interleukin (IL)10 deficiency through promoting growth of anti-inflammatory gut microbiota,¹⁷ and attenuating lipopolysaccharide (LPS)-induced inflammation through directly inhibiting Toll-like receptor 4 signaling in intestinal epithelial cells (IECs).¹⁸ Therefore, 2'-FL may have potential applications in maintaining intestinal homeostasis and preventing and/or treating intestinal diseases.

Chemotherapy and radiotherapy for patients with cancer have antineoplastic efficacy, owing to the cytotoxic effects on tumor cells. However, these therapeutics in the gastrointestinal tract lead to the severe complication of mucositis.¹⁹ Two clinical phenotypes of mucositis exist: oral mucositis in the upper digestive tract and intestinal mucositis predominantly in the small intestine. Mucositis occurs in 60%–100% of patients receiving high-dose chemotherapy and radiotherapy cancer treatments.²⁰ Clinical symptoms of mucositis include abdominal pain, bleeding, malnutrition, electrolyte imbalance, and severe infections.¹⁹ Therefore, the tolerance to mucositis is associated with patient compliance with completing the treatment regimens. A series of dynamic events are involved in the pathogenesis of mucositis. Antineoplastic therapies stimulate oxidative

stress, which in turn injures IECs and cells in the submucosa in the gastrointestinal tract. Signals from these injured cells trigger proinflammatory responses, such as activation of production of nuclear factor- κ B-mediated proinflammatory cytokines, including tumor necrosis factor (TNF) α , IL6, and IL1 β . These inflammatory responses further induce apoptosis, atrophy, ulceration, and inflammation in the gastrointestinal tract.^{19,21} From a therapeutic viewpoint, any steps in this pathologic process may serve as targets for management of intestinal mucositis. However, current management for mucositis largely involves symptom control. Limited mechanistic therapeutic agents are available for mucositis prevention and treatment.

The aim of this study was to investigate the roles of 2'-FL in the treatment of intestinal mucositis. The compound 5-fluorouracil (5-FU), an analogue to uracil, is an antimetabolite that inhibits cell proliferation and has been widely used for the treatment of a variety of tumors.^{22,23} Through in vitro assays, we have shown that 2'-FL has a direct effect in protecting IECs against 5-FU-induced apoptosis, but has no effect on 5-FU-treated cancer cells. The genomic analysis of the microbiome showed that 2'-FL plays roles in maintaining homeostasis of the gut microbiota community in mice treated with 5-FU. Thus, both effects of 2'-FL may contribute to prevention of 5-FU-induced mucositis. These results support the application of 2'-FL as a therapeutic strategy for preventing mucositis in cancer patients receiving chemotherapy.


Results

Treatment With 2'-FL Suppresses 5-FU-Induced Apoptosis in IECs but Has No Effect on Gastrointestinal Tumor Cells

Beyond their roles in nutrient absorption and the transportation of water and waste products, IECs lining the gastrointestinal tract provide the frontline response to components in the gut lumen in maintaining intestinal homeostasis.²⁴ The injury of IECs by 5-FU is a pathologic factor in the development of mucositis.^{19,21} Therefore, we first used in vitro assays to determine whether 2'-FL had direct effects in protecting IECs against 5-FU-induced injury.

The 2'-FU used in this study was synthesized by our group according to a previously described method²⁵ (Figure 1A). The purity of synthetic 2'-FL was examined

Abbreviations used in this paper: 2'-FL, 2'-fucosyllactose; 5-FU, 5-fluorouracil; EdU, 5-ethynyl-2'-deoxyuridine; ELISA, enzyme-linked immunosorbent assay; FBS, fetal bovine serum; FITC, fluorescein isothiocyanate; HMO, human milk oligosaccharide; IEC, intestinal epithelial cell; IL, interleukin; LPS, lipopolysaccharide; MPO, myeloperoxidase; mRNA, messenger RNA; MSIE, mouse small intestine epithelial cells; NMR, nuclear magnetic resonance; PBS, phosphate-buffered saline; PCR, polymerase chain reaction; SV40, simian virus 40; TNF, tumor necrosis factor; ZO-1, Zona occludin-1.

 Most current article

© 2021 The Authors. Published by Elsevier Inc. on behalf of the AGA Institute. This is an open access article under the CC BY-NC-ND license (<http://creativecommons.org/licenses/by-nc-nd/4.0/>).

2352-345X

<https://doi.org/10.1016/j.jcmgh.2021.09.015>

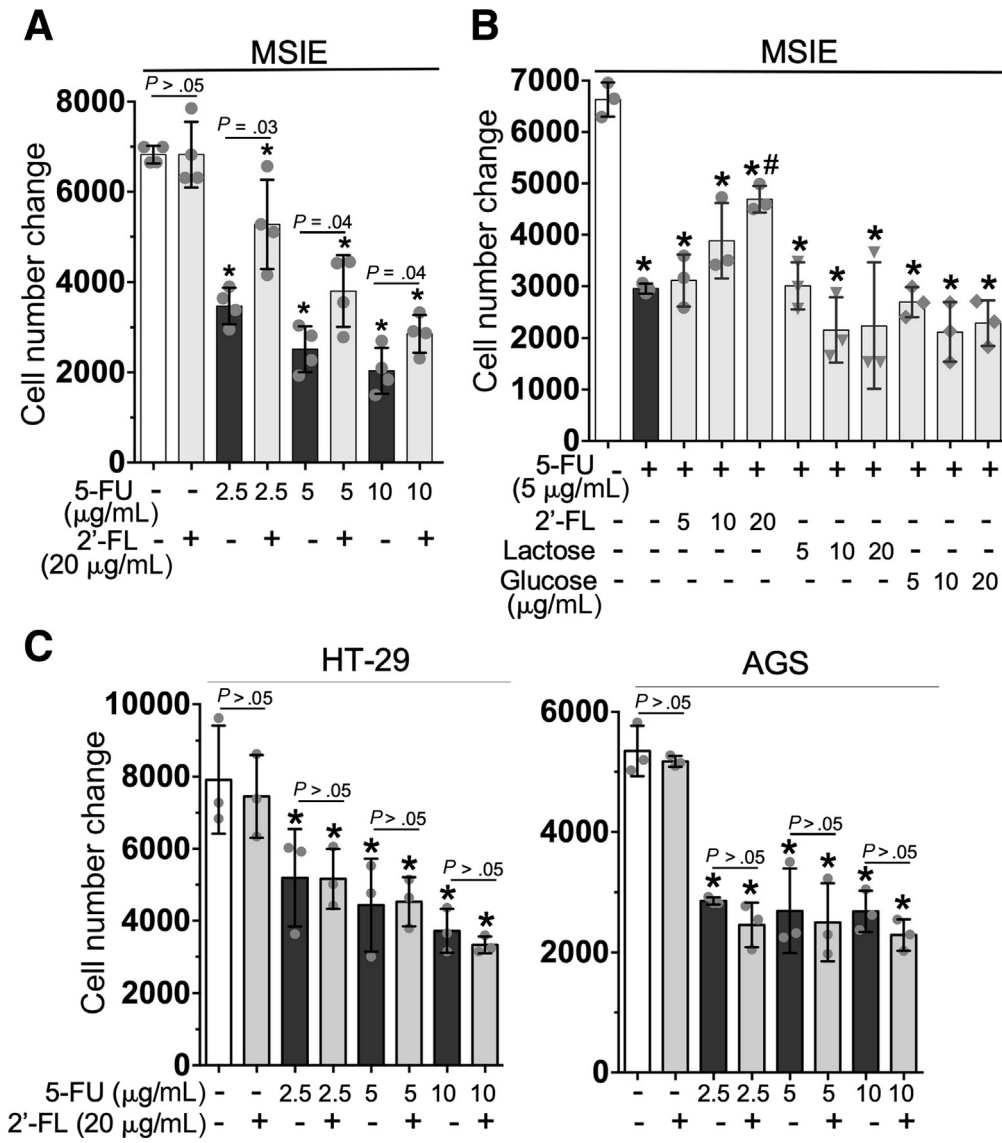


Figure 2. Treatment with 2'-FL mitigates the 5-FU-induced decrease in cell growth in small IECs but not in gastrointestinal tumor cells in vitro. (A and B) MSIE, (B) HT-29, and (D) AGS cells in 96-well plates were treated with 5-FU in the presence or absence of 2'-FL, α-lactose, or D-glucose at the indicated concentrations for 24 hours. Cell viability was assessed using the CellTiterH120 AqueousOne Solution Cell Proliferation Assay kit. The cell number change was calculated as follows: (cell number at the end of treatment - cell number before treatment [5000 cells/well]). **P* < .05 compared with the control group; #*P* < .05 compared with the 5-FU group. Each symbol represents data from 1 independent experiment.

(Figure 2A and B). Interestingly, the glycan controls, lactose and glucose, at the same concentrations as 2'FL did not affect the 5-FU-induced decrease in cell growth (Figure 2B), thus indicating the unique function of 2'-FL in IECs. Notably, 2'-FL did not affect the decrease in cell growth caused by 5-FU treatment in HT-29 and AGS cells (Figure 2C). These data provide novel evidence that 2'-FL blocks the cytotoxic effects of 5-FU in normal IECs, but not in tumor cells.

The metabolites of 5-FU inhibit cell division by suppressing the activity of thymidylate synthase, thus decreasing DNA synthesis and repair, and inducing cell death through incorporation into RNA.^{22,23} We next studied how 2'-FL promoted cell growth under the toxic influence of 5-FU. The effects of 2'-FL on apoptosis and proliferation in cells treated with 5-FU were tested in MSIE and tumor cells. The 5-FU treatment induced apoptosis in MSIE cells, as detected by Western blot analysis of a caspase-3 cleavage product; however, this effect was attenuated by 2'-FL co-

treatment in a concentration-dependent manner (Figure 3A). Interestingly, 5-FU did not induce apoptosis in AGS cells (Figure 3A). Apoptosis was further detected through Annexin V staining and flow cytometry. The increase in early apoptosis (Annexin V⁺PI⁻ cells) in 5-FU-treated MSIE cells was decreased significantly by 2'-FL (Figure 3B and C). To examine the contribution of apoptosis to the 5-FU-regulated loss of cell growth in MSIE cells, we treated cells with a caspase inhibitor, zVAD-fmk, which restored 5-FU-induced cell loss in MSIE cells (Figure 3D). Furthermore, immunostaining of enteroids showed that 5-FU treatment increased the number of cells with positive staining of cleavage caspase-3 and E-cadherin (an epithelial cell adherent junctional marker), which was suppressed by 2'-FL co-treatment. This result indicates that 2'-FL inhibits 5-FU-stimulated apoptosis in epithelial cells in enteroid cultures (Figure 3E). Thus, blocking of apoptosis in intestinal epithelial cells by 2'-FL has the potential for alleviating 5-FU-induced loss of normal IECs.

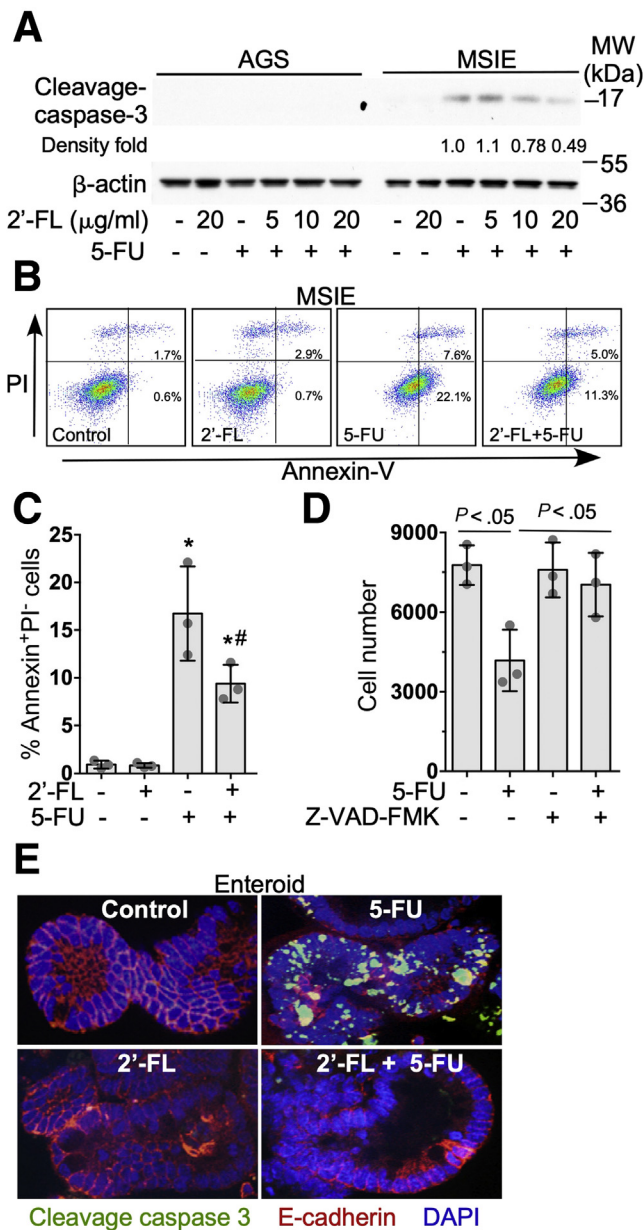


Figure 3. Treatment with 2'-FL suppresses 5-FU-induced apoptosis in small IECs in vitro. (A) MSIE and AGS cells were treated with 5-FU (10 μ g/mL) for 6 hours with or without co-treatment with 2'-FL at the indicated concentrations. Total cellular proteins were prepared for Western blot analysis with anti-cleavage-caspase 3 antibody; β -actin blot was used as the protein loading control. The fold changes of band density compared with the 5-FU-treated sample are shown under the blot. (B and C) MSIE were treated with 5-FU (10 μ g/mL) for 24 hours in the presence or absence of 2'-FL (20 μ g/mL). Cells were stained with FITC-Annexin and propidium iodide (PI) for flow cytometry. (B) Representative density plots with FITC-Annexin vs PI and percentages of cells in early apoptosis (Annexin V⁺PI⁺) are shown. (D) MSIE cells in 96-well plates were treated with 5-FU (10 μ g/mL) in the presence or absence of a cell-permeable caspase inhibitor, Z-VAD-FMK (20 μ mol/L), for 24 hours. Cell viability assays and the cell number change calculation are described in Figure 2. (E) Wild-type enteroids were treated with 5-FU in culture medium (10 μ g/mL) for 6 hours with or without 2'-FL (20 μ g/mL)

Cell proliferation generally is controlled by the progression of 3 distinctive phases

of the cell cycle (G0/G1, S, and G2/M), and cell-cycle arrest is considered one of the most common causes of the inhibition of cell proliferation. Based on the data that 2'-FL at 20 μ g/mL inhibited 5-FU-induced inhibition of cell growth in MSIE cells (Figure 2A and B), we chose this concentration of 2'-FL to detect the effects of 2'-FL on proliferation in MSIE and HT-29 cells treated with 5-FU. Cells were labeled with 5-ethynyl-2'-deoxyuridine (EdU) and propidium iodide to detect cell-cycle progression by flow cytometry. In agreement with previously reported evidence that 5-FU induces S-phase arrest in tumor cells,²⁶ we found that 5-FU treatment resulted in a characteristic S-phase arrest, with a greater number of cells in S phase and fewer cells in G2 phase, in both MSIE and HT-29 cells. However, 2'-FL co-treatment did not affect S-phase arrest induced by 5-FU in either MSIE or HT-29 cells (Figure 4), thus suggesting that 2'-FL does not affect the 5-FU-induced inhibition of proliferation in normal IECs and tumor cells.

Therefore, these data suggest that 2'-FL protects normal IECs against 5-FU-induced injury through alleviating apoptosis. However, 5-FU-induced inhibition of proliferation in tumor cells and normal IECs is not affected by 2'-FL.

Pretreatment With 2'-FL Ameliorates 5-FU-Induced Intestinal Mucositis in Mice

Experimental studies have shown that the mouse model of intestinal mucositis induced by 5-FU shows intestinal epithelial damage and inflammatory responses in the small intestine.²⁷ We used this mouse mucositis model to investigate the effects of 2'-FL on intestinal mucositis. Mice were injected peritoneally with 5-FU to induce mucositis and were killed 3 days after injection (5-FU-3D group). Mice were given 2'-FL in drinking water 4 days before (pretreatment, 5-FU-3D-2'-FL-7D group) or concurrently (concurrent treatment, 5-FU-3D-2'-FL-3D group) with 5-FU injection. Mice receiving phosphate-buffered saline (PBS) injection were used as controls (Figure 5A). No significant body weight changes were identified in control mice. We observed that the percentages of body weight compared with the original body weight on days 1, 2, and 3 after 5-FU injection were 94.54% \pm 1.39%, 90.81% \pm 1.72%, and 88.07% \pm 1.63%, respectively, in the 5-FU-treated group, and 95.69% \pm 1.27%, $P < .05$; 93.83% \pm 0.96%, $P < .05$; and 92.86% \pm 1.62%, $P < .05$, respectively, in the 2'-FL

pretreatment for 24 hours. 2'-FL was present during 5-FU treatment. Enteroids were prepared for immunostaining to detect apoptosis using rabbit anti-cleavage-caspase 3 antibody and FITC-conjugated secondary antibody (green) and an epithelial cell marker using mouse anti-E-cadherin antibody and Cy3-conjugated secondary antibody (red). Nuclei were stained with 4',6-diamidino-2-phenylindole (DAPI) (blue). (A and E) Data are representative of at least 3 independent experiments. (C) * $P < .05$ compared with the control group; # $P < .05$ compared with the 5-FU group. (C and D) Each symbol represents data from 1 independent experiment.

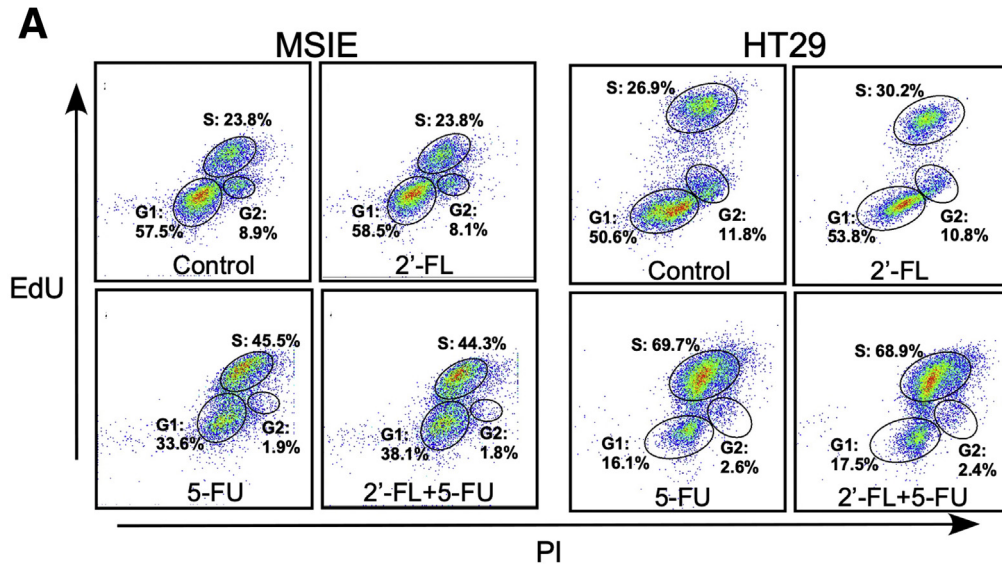


Figure 4. Treatment with 2'-FL does not affect 5-FU-induced cell-cycle arrest in small IECs and in gastrointestinal tumor cells in vitro. MSIE cells and HT-29 cells were treated with 5-FU (10 $\mu\text{g}/\text{mL}$) with and without co-treatment with 2'-FL (20 $\mu\text{g}/\text{mL}$) for 24 hours. Cell proliferation was detected by EdU labeling and staining with FITC-conjugated anti-EdU antibody and propidium iodide staining for flow cytometry. (A) Representative density plots of FITC-EdU vs propidium iodide are shown. (B) The percentages of cells in G1, S, and G2 phase are shown. * $P < .05$ compared with the same phase of the control group. Data represent results from 3 separate experiments.

MSIE				
	Control	2'-FL	5-FU	2'FL+5-FU
G1	57.5 \pm 2.9%	60.9 \pm 5.6%	30.8 \pm 6.1%*	37.9 \pm 7.9%*
S	24.2 \pm 3.5%	24.5 \pm 4.1%	40.8 \pm 5.7%*	48.9 \pm 4.3%*
G2/M	8.9 \pm 1.0%	8.4 \pm 1.6%	3.0 \pm 1.7%*	3.2 \pm 1.6%*

HT-29				
	Control	2'-FL	5-FU	2'FL+5-FU
G1	50.2 \pm 2.4%	53.3 \pm 1.5%	19.8 \pm 3.8%*	19.6 \pm 2.2%*
S	24.1 \pm 2.7%	28.4 \pm 4.7%	67.3 \pm 5.5%*	64.5 \pm 4.1%*
G2/M	14.1 \pm 2.4%	10.5 \pm 2.9%	3.3 \pm 1.4%*	3.2 \pm 0.9%*

pretreatment group. Thus, 5-FU-treated mice began to lose body weight the first day after 5-FU injection, and the body weight loss continued until the mice were killed on the third day after 5-FU injection. Pretreatment with 2'-FL significantly mitigated body weight loss from day 1 to day 3 (Figure 5B). Compared with the 5-FU-treated group, no significant difference in body weight change was observed in the concurrent treatment group (93.79% \pm 1.99%, $P > .05$; 91.76% \pm 1.55%, $P > .05$; and 89.46% \pm 3.17%, $P > .05$ for body weight on days 1, 2, and 3 after 5-FU injection vs original body weight, respectively).

As reported before, 5-FU-treated mice showed ulceration and inflammatory cell infiltration in the small intestine. These abnormalities were decreased by 2'-FL pretreatment (Figure 5C). Villus shortening is a characteristic of intestinal mucositis.²⁷ Compared with control cells, 5-FU-treated cells showed blunted villi (225.2 \pm 17.8 vs 107.4 \pm 19.8 μm , respectively; $P < .0001$). The 2'-FL pretreatment (172.5 \pm 28.1 μm ; $P < .0001$), but not concurrent treatment (122.1 \pm 19.6 μm ; $P > .05$), alleviated 5-FU-induced shortening of villi (Figure 5D).

To examine 5-FU-induced intestinal injury and inflammation, we killed mice 1 day (5-FU-1D) or 3 days (5-FU-3D)

after 5-FU injection with either 2'-FL pretreatment (5-FU-1D-2'-FL-5D, 5-FU-3D-2'-FL-7D) or concurrent treatment (5-FU-1D-2'-FL-1D, 5-FU-3D-2'-FL-3D) (Figure 6A). In the small intestine in 5-FU-treated mice, the inflammatory scores on the first and third days after 5-FU injection were 5.8 \pm 0.84 and 8.43 \pm 0.96, respectively (Figure 6B). The 2'-FL pretreatment significantly decreased inflammation scores (4.37 \pm 0.52, $P < .001$ on the first day, and 6.9 \pm 1.1, $P < .001$ on the third day) (Figure 6B). Increased pro-inflammatory cytokine production is a hallmark of chemotherapy-induced mucositis.¹⁹ Therefore, we tested the effects of 2'-FL on inflammatory cytokine production in the 5-FU-induced mucositis model. We used real-time polymerase chain reaction (PCR) analysis of RNA isolated from the small intestinal tissues to detect messenger RNA (mRNA) levels of proinflammatory cytokines. We found that the 2'-FL pretreatment down-regulated the 5-FU-induced mRNA levels of TNF ($P < .05$) on the first and third days after 5-FU injection (Figure 6C). Neutrophil infiltration in inflammatory tissue results in increased release of myeloperoxidase (MPO). MPO levels in the small intestinal tissue lysates were examined using the mouse MPO enzyme-linked immunosorbent assay (ELISA) kit. Inconsistent with the

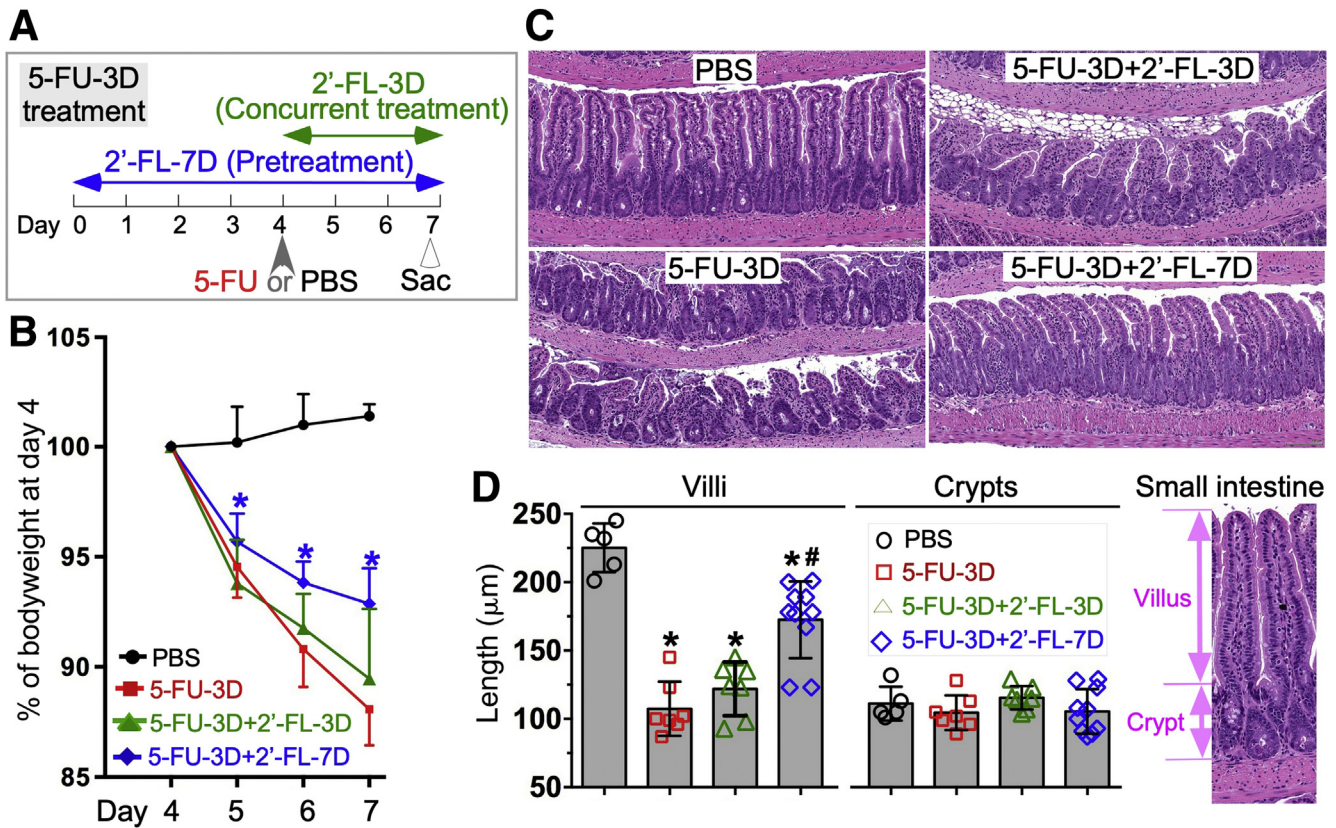


Figure 5. Pretreatment with 2'-FL alleviates 5-FU-induced body weight loss and shortening of villi in mice. (A) The treatment plan. Wild-type C57BL/6J mice received 2'-FL supplementation in drinking water (1 mg/mL) 4 days before (pretreatment) or concurrently with induction of intestinal mucositis by intraperitoneal injection of 5-FU in PBS (250 mg/kg body weight). Control mice were injected with PBS. Mice were killed on the third day after 5-FU injection. (B) Body weight was recorded. The fold change in body weight was calculated by comparing the body weight at the indicated day with that of the same mouse on day 4. (C) The ileal tissue sections were stained with H&E. (D) The lengths of villi and crypts are shown. (B) * $P < .05$ compared with the control group on the same day of treatment. $N = 5-10$ in each group. (D) * $P < .05$ compared with the control group; # $P < .05$ compared with the 5-FU-treated group. The symbol represents data from 1 mouse. Sac, Sacrifice.

results of the inflammatory score, 5-FU up-regulated MPO levels in the small intestine on the first and third day after 5-FU injection, which were alleviated by 2'-FL pretreatment (Figure 6D).

In this study, there were no changes in crypt length in 5-FU-treated mice (Figure 5C and D). The inflammatory scores in the colon in mice on the first and third day after 5-FU injection, with or without pretreatment or concurrent treatment, were less than 2. These results indicate that the colon might not be the target of 5-FU-induced inflammation, in agreement with previous evidence that intestinal mucositis occurs in the small intestine.²⁰

We next examined the effects of 2'-FL on protecting intestinal integrity in this model of mucositis. Treatment with 5-FU induced small intestinal epithelial cell apoptosis on the first day after injection (5-FU-1D group), as detected with an in situ oligo ligation kit, and was inhibited by 2'-FL pretreatment (Figure 7A and B). The mucus layer plays an important role in protecting epithelial surfaces against bacterial and viral assault and mechanical damage in the gastrointestinal tract.^{28,29} Goblet cells are mucin-producing cells. The goblet cell number in the small intestine has

been reported to decrease in mice after 5-FU treatment.³⁰ In agreement with this evidence, Mucin 2 (MUC2) immunostaining showed fewer Goblet cells in the small intestine in mice after 5-FU treatment (5-FU-3D group), an effect that was attenuated significantly by 2'-FL pretreatment (Figure 7C and D). As a marker of tight junction structure, Zona occludin-1 (ZO-1) normally localizes in the apical tight junctional complexes in cells that play roles in preserving the tight junction stability and epithelial barrier function.³¹ We determined the distribution of ZO-1 in cells using immunostaining. 5-FU induced redistribution of this protein from the apical surface to the cytoplasmic compartment of small intestinal epithelial cells (5-FU-3D group). The apical surface localization of ZO-1 was observed in the 2'-FL pretreatment group (Figure 7E). This evidence indicates that 2'-FL pretreatment plays a role in preserving intestinal integrity.

Notably, our results suggest that 2'-FL concurrent treatment is less effective than 2'-FL pretreatment against 5-FU-induced mucositis in mice. 2'-FL concurrent treatment had significant effects in decreasing small epithelial cell apoptosis on the first day after 5-FU injection ($P < .05$)

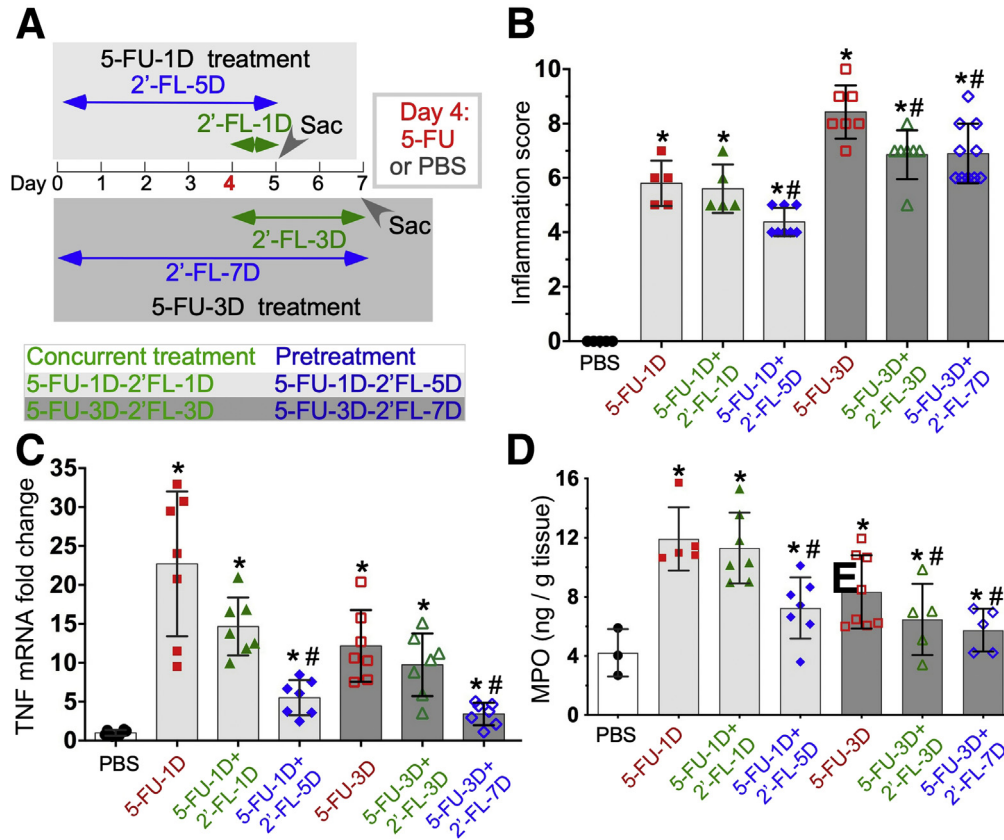


Figure 6. Pretreatment with 2'-FL decreases 5-FU-induced inflammation in the small intestine in mice. (A) The treatment plans are shown. Mice were treated as described in Figure 5 and were killed on the first or third day after 5-FU injection. (B) The inflammation scores are shown. (C) Real-time PCR analysis was performed to detect TNF gene expression in the small intestinal mucosa. The average mRNA expression levels in control mice were set as 100%, and the mRNA expression level of each mouse was compared with the average. (D) The MPO levels in the small intestinal tissues were examined. * $P < .05$ compared with the PBS group; # $P < .05$ compared with the 5-FU-treated group in the same treatment plan. (B–D) Each symbol represents data from 1 mouse. Sac, Sacrifice.

(Figure 7A and B) and decreasing the inflammatory score (6.86 ± 0.90 , $P < .001$) (Figure 6B) and the MPO level ($P < .05$) (Figure 6D) on the third day after 5-FU injection. However, 2'-FL concurrent treatment did not have any effects on 5-FU-induced body weight loss (Figure 5B) and villus shortening (Figure 5C), inflammation (inflammatory score, 5.6 ± 0.89 ; $P > .05$) (Figure 6B), and the MPO level (Figure 6D) on the first day after 5-FU injection, and TNF production (Figure 6C) on the first and third day after 5-FU injection. These results suggest that 2'-FL pretreatment is required for protecting the intestinal epithelium against 5-FU-induced injury.

In agreement with the in vitro data indicating that 2'-FL did not affect 5-FU-induced S-phase arrest in MSIE, the number of proliferative cells with Ki67-positive staining were diminished in the small intestine in 5-FU-treated mice with or without 2'-FL pretreatment or concurrent treatment (Figure 8). These data suggest that 2'-FL does not block the inhibitory effect of 5-FU on cell proliferation. Instead, 2'-FL pretreatment supports intestinal integrity, thereby protecting against 5-FU-induced injury through ameliorating 5-FU-stimulated apoptosis.

2'-FL Decreases 5-FU-Induced Alteration of the Intestinal Microbiota Composition in Mice

It has been reported that chemotherapy is associated with dysbiosis in patients³² and in animal models of mucositis.³³ 2'-FL has shown beneficial effects on the gut microbiota community in adulthood¹⁶; therefore, we examined the impact of 2'-FL on the gut microbiota community in mice treated with 5-FU. Community profiling of the fecal bacteria from mice killed 3 days after 5-FU injection with and without 2'-FL pretreatment or concurrent treatment (treatment plan in Figure 5A) and mice receiving 2'-FL for 7 days (2'-FL-7D) was analyzed by high-throughput genomic sequencing. The overall fecal bacterial composition, such as β -diversity, was measured by weighted UniFrac distance using family level bacterial abundance data, and principal coordinate analysis was performed to compare similarities in bacterial composition across the 5 groups. Permutational multivariate analysis of variance showed significant separation of the 5-FU-3D group from the control group ($P = .011$) and the 2'-FL pretreatment group ($P = .04$). In addition, the 2'-FL pretreatment group was significantly different from the control group ($P = .001$)

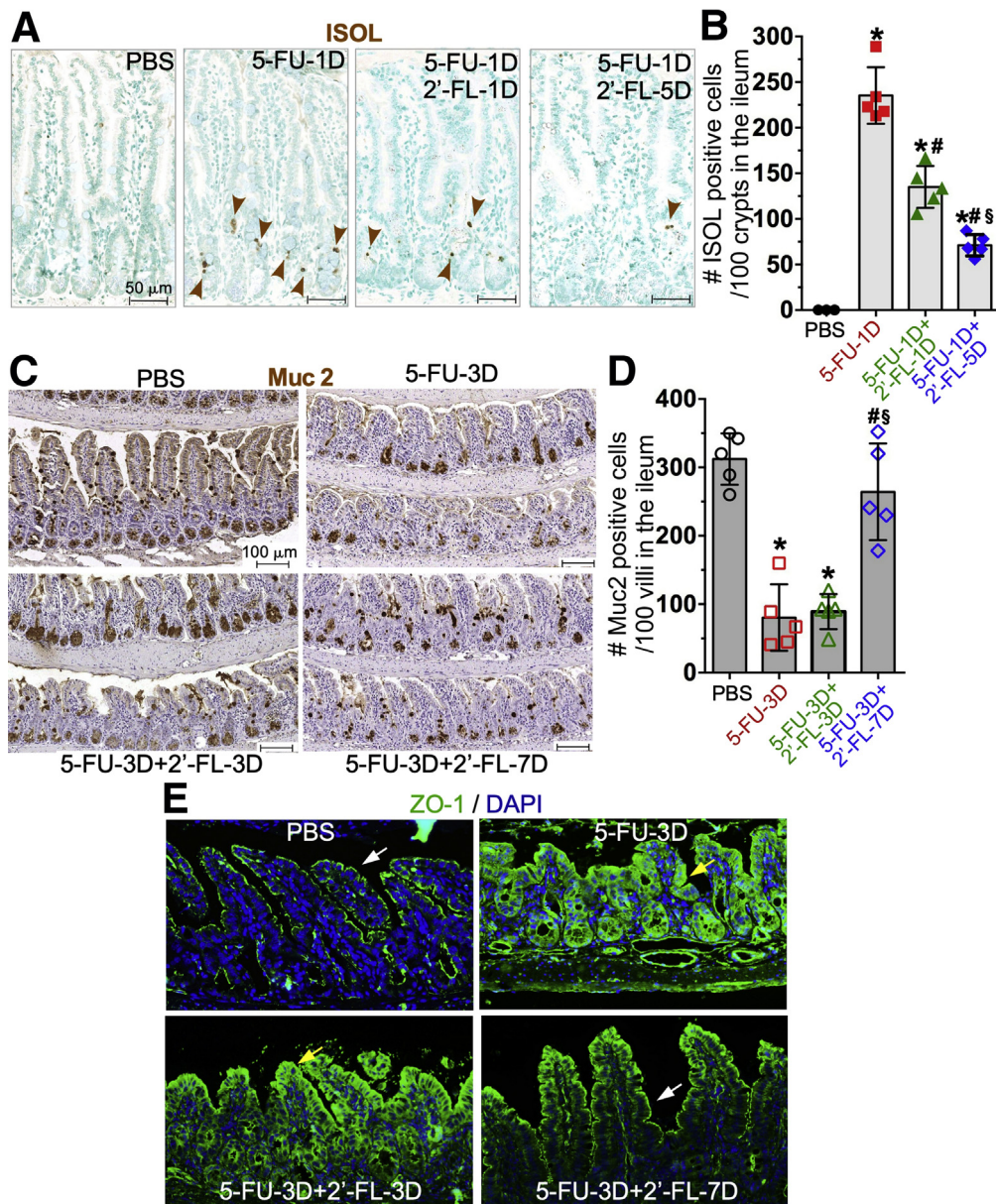


Figure 7. Pretreatment with 2'-FL protects against 5-FU-induced injury in the small intestine in mice. Mice were treated as described in Figure 5 and were killed on the first or the third day after 5-FU injection, as shown in Figure 6A. (A) Apoptosis in ileal tissues was detected with in situ oligo ligation (ISOL) assays. Sections were counterstained with methyl green. (B) The number of positive ISOL cells is shown. (C) Ileal tissue sections were immunostained with anti-Muc2 antibody and a horse-radish-peroxidase-conjugated secondary antibody. Slides were developed with 3,3'-diaminobenzidine tetra hydrochloride and counterstained with hematoxylin. (D) The number of positively stained Muc2 cells is shown. (E) Ileal tissue sections were stained with an anti-ZO-1 antibody and a FITC-labeled secondary antibody (green). Nuclei were stained with 4',6-diamidino-2-phenylindole (DAPI) (blue). Membrane (white arrows) and intracellular (yellow arrows) ZO-1 distribution are shown. Slides were scanned and images were exported at 10 \times magnification for bright-field images and 20 \times magnification for florescent images. Images in this figure represent results from at least 3 mice in each group. (B and D) * $P < .05$ compared with the control group; # $P < .05$ compared with the 5-FU-treated group; § $P < .05$ compared with the 2'-FL concurrent treatment group. Each symbol represents data from 1 mouse.

and the 2'-FL concurrent treatment group ($P = .038$). No segregation was observed between the control and 2-FL-7D groups ($P = .192$) and between the 5-FU-3D and 2'-FL concurrent treatment groups ($P = .138$) (Figure 9A). α -diversity indexes (Shannon and Simpson) were unchanged among the 5 groups (Figure 9B). Examination of the

abundance of the fecal microbiota identified 18 specific taxa at the family level with a relative abundance greater than 0.1%. 5-FU-treated mouse fecal microbiota had a significant expansion ($P < .05$) in Helicobacteraceae, Bacteroidaceae, and Deferribacteraceae, and a reduction in Lactobacillaceae and Muribaculaceae, as compared with the control group

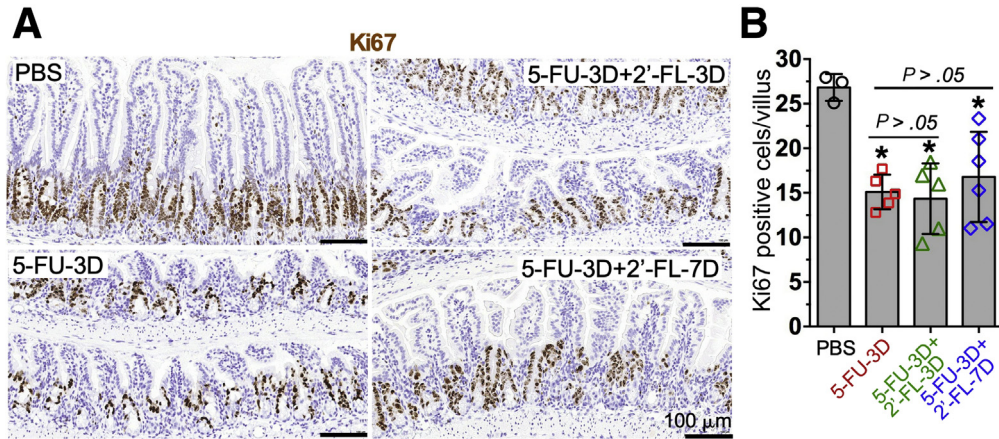


Figure 8. Inhibition of cell proliferation in the small intestine by 5-FU is not altered by 2'-FL pretreatment in mice. Mice were treated as described in Figure 5 and were killed on the third day after 5-FU injection, as shown in Figure 5A. (A) Ileal tissues were immunostained with an anti-Ki67 antibody and a horseradish-peroxidase-conjugated secondary antibody. Slides were developed with 3,3'-diaminobenzidine tetra hydrochloride and counterstained with hematoxylin. (B) The number of positively stained cells is shown. * $P < .05$ compared with the control group. Each symbol represents data from 1 mouse.

(Figure 9C). 2'-FL pretreatment and concurrent treatment significantly decreased the 5-FU-induced expansion of Helicobacteraceae. The reduction of Lactobacillaceae by 5-FU was mitigated by 2'-FL pretreatment, but not concurrent treatment. The other 3 altered families by 5-FU were not affected by 2'-FL pretreatment or concurrent treatment (Figure 9C). We further analyzed detailed abundance analysis of the major taxonomic groups at the species level within these five 5-FU-altered families. Our results showed that the abundances of up-regulated *Helicobacter ganmani* and down-regulated *Lactobacillus murinus* by 5-FU treatment were alleviated significantly by 2'-FL pretreatment. Concurrent treatment only alleviated the 5-FU-induced increase in *Helicobacter ganmani*. The alterations of the abundances of other species, *Muribaculum intestinale*, *Bacteroides sartorii*, and *Mucispirillum schaedleri*, by 5-FU were not affected by 2'-FL pretreatment or concurrent treatment (Figure 9D). Thus, these results suggest that 2'-FL pretreatment and concurrent treatment elicited a partial shift of the composition of the gut microbiota in 5-FU-treated mice toward normal levels. Therefore, prevention of 5-FU-induced intestinal mucositis by 2'-FL may be associated with the effects of 2'-FL in improving the 5-FU-driven imbalance of the gut microbiota community in mice.

Discussion

Chemotherapy and radiotherapy suppress tumor cell growth; however, these treatments injure normal cells in the gastrointestinal tract, thus resulting in mucositis. The outcomes of mucositis are highly associated with decreased quality of life and interruption of cancer treatment.³⁴ Currently available therapeutic agents to manage intestinal mucositis are limited. The potential approaches to treat mucositis independently of cancer treatment may include targeted interventions to block the pathogenesis of mucositis, such as through scavenging reactive oxygen species,

suppressing proinflammatory cytokine production or function, and inhibiting apoptosis.²¹ Remarkably, the results from this work showed a novel effect of 2'-FL in mitigating 5-FU-stimulated apoptosis in normal IECs. Treatment with 2'-FL ameliorated 5-FU-induced intestinal mucositis by protecting the intestinal epithelium against injury. Importantly, 2'-FL did not affect 5-FU-induced cell loss in gastrointestinal tumor cells. Furthermore, we did not identify an effect of 2'-FL on 5-FU-induced inhibition of proliferation in both normal IECs and tumor cells. Therefore, 2'-FL may serve as a cytoprotective agent to increase the ability of patients to tolerate the complications of chemotherapy without comprising the efficacy of therapeutic treatments for cancer.

It has been reported that HMOs exert direct effects on modulating cellular responses. HMOs have been shown to regulate the expression of genes involved in immune responses in human fetal intestinal mucosa in an ex vivo experiment.³⁵ Previous studies also observed several direct effects of 2'-FL in immature intestinal epithelial cell lines. For example, 2'-FL promoted cell differentiation³⁶ and inhibited inflammatory responses by suppressing the expression of CD4, a member of the LPS-receptor complex, thus decreasing LPS-induced inflammatory responses¹⁸ and attenuating TNF-induced inflammation.³⁷ This evidence from immature intestinal epithelial cells supports the potential function of 2'-FL in direct promotion of intestinal development and the maturation of the immune system in the early stage of life. This study identified a previously unrecognized direct effect of 2'-FL on the inhibition of 5-FU-induced apoptosis in normal mature IECs. However, currently, the mechanisms involved in the direct interaction of 2'-FL and IECs that leads to regulation of the function of IECs remain unclear. Glycosylation of proteins plays an important role in protein folding and biological recognition of other molecules.³⁸ We speculate that 2'-FL has the potential to directly interact with cell surface proteins, such as

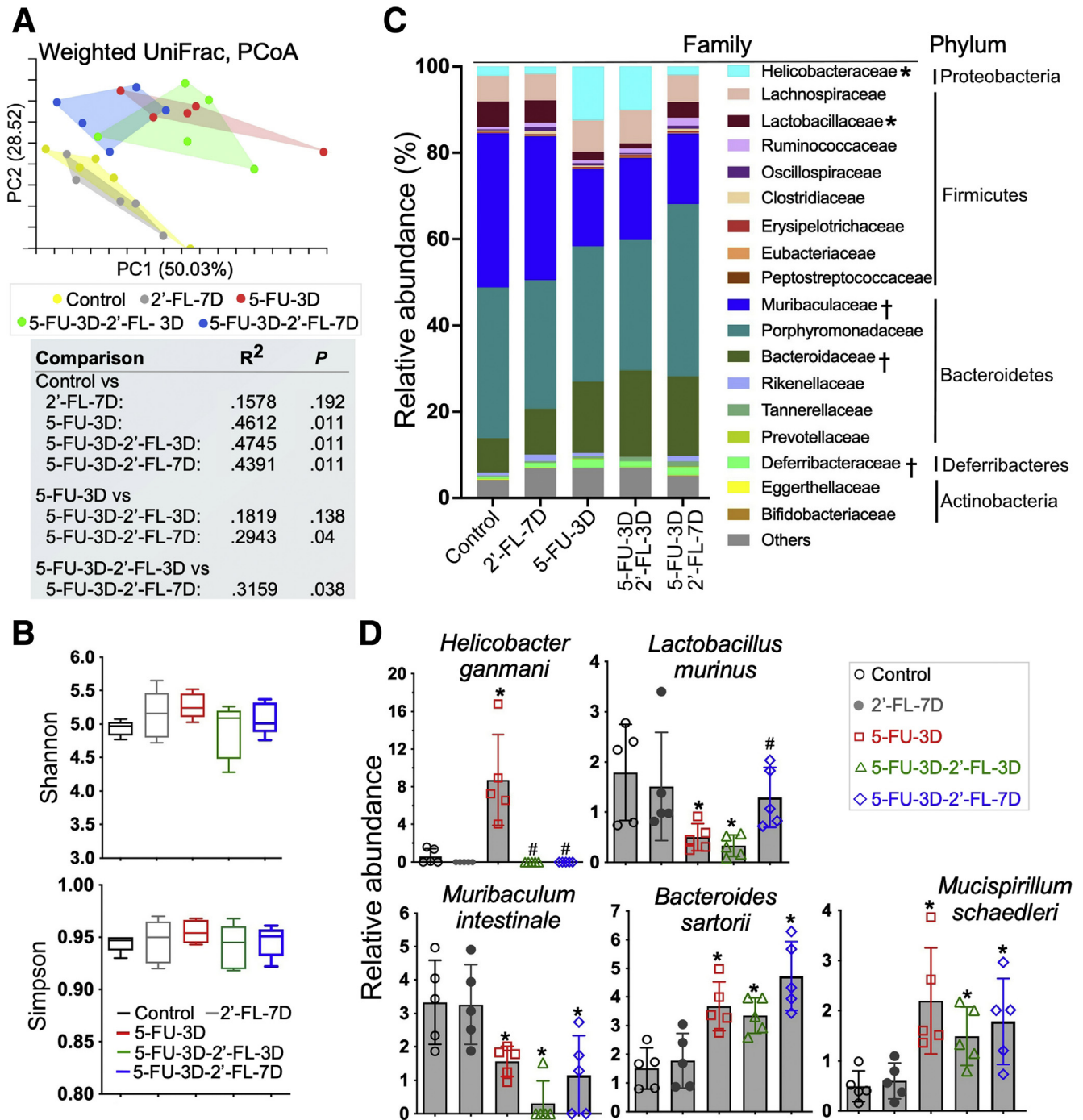


Figure 9. 2'-FL restores 5-FU-altered fecal gut microbiota composition in mice. Wild-type C57BL/6J mice received 5-FU with or without 2'-FL co-treatment as described in Figure 5. Mice in the 2'-FL-7D group received 2'-FL for 7 days only. Feces were collected at the end of treatment and fecal RNA was isolated for high-throughput genomic sequencing. (A) Principal coordinate analysis. R² and P values for comparison of the indicated groups are shown. (B) α -diversity analysis. There were no significant changes of Shannon and Simpson among the 5 groups ($P > .05$). (C) The relative abundance of bacterial reads classified at the family level. Families with a relative abundance greater than 0.1% are presented. Families with a relative abundance less than 0.1% and unidentified families were grouped into "others." Each bar represents the average relative abundance of each group. $n = 5$ in each group. * \dagger Relative abundance of these families was altered significantly by 5-FU treatment ($P < .05$). *Families were restored toward the control levels by 2'-FL pretreatment ($P < .05$). \dagger 2'-FL pretreatment had no effect on the families. (D) The top relative abundance of the species within the family altered by 5-FU is shown. * $P < .05$ compared with the control group; # $P < .05$ compared with the 5-FU-3D group.

receptors, to manipulate their structural conformation and interactions with other receptors, resulting in modulating their biological activities and downstream signaling pathways and cellular responses. This area of research is worthy of future study.

The effects of HMOs on tumor cells have been investigated, and several studies have reported inhibition of proliferation and induction of apoptosis by 2'-FL³⁶ and 2'-FL containing neutral HMO fractions³⁹ in gastrointestinal tumor cells. However, another study has found that apoptosis is induced by neutral HMO fractions, but proliferation is inhibited by neutral and acidic HMO fractions, except for fucosyllactose, in HT-29 and Caco-2 cells.³⁹ Our study did not identify any significant effects of 2'-FL alone on cell growth, apoptosis, and proliferation in normal mature IECs and tumor cells. These differing results may be owing to the various concentrations of 2'-FL used and the treatment periods applied for cell treatment. In the previous studies, 2'-FL at concentrations higher than 200 $\mu\text{g}/\text{mL}$ for 72 hours was used to inhibit cell proliferation and increase differentiation in HT-29 and well-differentiated Caco-2Bbe cells.³⁶ In contrast, the highest dose of 2'-FL used in this study was 20 $\mu\text{g}/\text{mL}$ for 24 hours. This low concentration of 2'-FL suppressed 5-FU-induced apoptosis in normal IECs, and high concentrations of 2'-FL inhibited proliferation and induction of apoptosis in tumor cells. These findings underscore the potential for using 2'-FL to prevent mucositis, through the protection of normal IECs and inhibition of tumor growth.

HMOs are well-known prebiotics modulating the symbiotic relationship between the gut microbiota and the host in early life.^{10,11} 2'-FL promotes the growth of bifidobacteria and metabolite production in feces from infants.¹⁵ A parallel, double-blind, randomized, placebo-controlled clinical study has shown that 2'-FL supplementation is safe and well tolerated, and regulates the gut microbiota profile by increasing Actinobacteria and Bifidobacterium and decreasing Firmicutes and Proteobacteria in adults.¹⁶ Thus, we further investigated the impact of 2'-FL on the gut microbiota community in mice with 5-FU-induced colitis. The disruption of homeostasis of the intestinal microbiota is associated with intestinal inflammatory diseases.⁴⁰ The previous studies have identified dysbiosis in mucositis, such as a decrease in protective bacteria, *Lactobacillus*, and an increase in pathogens.^{30,33} In agreement with this evidence, we showed that 5-FU treatment down-regulated an abundance of bacteria that have shown beneficial effects on inhibition of mucositis, such as *Lactobacillus* species⁴¹ and *Muribaculum* species⁴² in mice, and up-regulated an abundance of bacteria that are associated with gastrointestinal inflammation, such as *Helicobacter* species, which has a strong association with intestinal inflammatory disease diseases in patients.⁴³ The roles of *B. sartorii* and *M. schaedleri* that were regulated by 5-FU in mucositis remain unclear. We also found that 2'-FL inhibited *Helicobacter* and restored *Lactobacillus* in 5-FU-treated mice. These results support the roles of 2'-FL in maintaining the homeostasis of the gut microbiome against 5-FU-induced dysbiosis, which may contribute to ameliorating mucositis. It should be noted

that the microbiota community profile in the 2'-FL-7D group is the same as that of the control group. Because 2'-FL concurrent treatment has less effects on mucositis, as compared with pretreatment, the longer time with 2'-FL treatment may exert a stronger impact on the gut microbiota.

Furthermore, impediments in HMO research and application center on the limited availability of sources to obtain heterogeneous HMOs. Indeed, the procedures to isolate and purify individual oligosaccharides from the 200 unique oligosaccharides present in breast milk are complex and intractable. Although the chemical synthesis of 2'-FL is obsolete at industrial levels,⁴⁴ in which kilogram syntheses are possible with whole-cell production, we were able to use organic synthesis to produce 2'-FL at the gram scale with significantly higher purity. The approach used in this work thus may provide a basis to produce clinical grade 2'-FL. Moreover, successful synthesis of 2'-FL is necessary to enable the development of this product and related tool molecules (such as fluorescently labeled 2'-FL) for biological studies and clinical applications in the future.

In summary, studies from this work elucidate a novel effect of 2'-FL on the inhibition of intestinal epithelial cell apoptosis and maintaining the balance of the gut microbiota community, thereby preventing 5-FU-induced mucositis. Extending previously reported nutritional application in early life,¹⁴ herein we show the protective effects of 2'-FL in adulthood. Notably, this knowledge should provide mechanistic insights to support interventions with 2'-FL as a strategy for maintaining intestinal health during chemotherapy-induced mucositis.

Materials and Methods

Synthesis of 2'-FL and Purity Detection

We synthesized 2'-FL according to a previously reported method for preparation of 2'-FL at the kilogram level.²⁵ Briefly, a fucosyl thioglycoside was converted to its bromide by the addition of elemental bromine (Br_2) at 5°C in dichloromethane. Excess Br_2 was removed through the addition of cyclohexene. A combined solution of the lactose acceptor and tetrabutylammonium bromide in dimethylformamide was added to the crude solution of fucosyl bromide, and the reaction mixture was stirred for 48 hours. Next, the reaction mixture was treated with sodium methoxide in methanol for 6 hours, and with 80% of acetic acid in water at 80°C for 12 hours. The crude material was crystallized from ethyl acetate and purified by recrystallization from methanol. The final intermediate was obtained after hydrogenation in 85% yield.

Synthetic 2'-FL was characterized by ^1H and ^{13}C NMR and high-resolution mass spectrometry to determine the purity of the compound. NMR spectra were recorded on a Bruker spectrometer (Bruker Corporation, Billerica, MA) in deuterated solvents. NMR spectra acquired in a mixture of deuterated solvents were calibrated to the residual solvent peaks of the more abundant solvent. NMR data were analyzed in TopSpin software (Bruker Corporation).

Spectrometric data of 2'-FL in ^1H NMR (400 MHz, D_2O) included the following: δ 5.27 (d, H-1'), 5.18 (d, J_{1,2} 3.3 Hz, H-1 α), 4.60 (d, J_{1,2} 7.7 Hz, H-1 β), 4.48 (d, J_{1,2} 7.6 Hz, H-1'),

4.21 (m, J_{5,6} 6.5 Hz, H-5''), 3.79 (d, J_{2,3} 9.8 Hz, H-2''), 3.25 (dd, J_{1,2} 7.7 Hz, H-2 β), 1.19 (d, J_{5,6} 6.5 Hz, H-6''). Spectrometric data of 2'-FL in ¹³C NMR (100 MHz, D₂O) included the following: δ 102.5 (C-1'), 101.6 (C-1''), 98.2 (C-1 α), 94.1 (C-1 β), 78.6 (C-4 α), 78.4 (C-4 β), 78.2 (C-3''), 77.5 (C-5''), 76.6 (C-3 β), 76.6 (C-5 β), 76.2 (C-3'), 75.9 (C-2''), 74.8 (C-4''), 73.9 (C-3 β), 73.6 (C-2 β), 71.9 (C-2 α), 71.4 (C-5'), 71.4 (C-5 α), 70.5 (C-2''), 69.2 (C-4'), 62.5 (C-6 β), 62.4 (C-6 α), 61.9 (C-6'), and 17.5 (C-6''). All signals identified in the ¹H and ¹³C NMR spectra represent a unique hydrogen atom or carbon atom of 2'-FL. No additional signals that could be attributed to impurities were identified in ¹H or ¹³C NMR. (d: doublet; dd: doublet of doublets; H: proton; J: the coupling constant)

Cell Culture

The MSIE cell line was generated from the small intestines of immortalized mice (Immortomice), which harbored thermolabile simian virus 40 (SV40) large tumor antigen from a SV40 strain, tsA58.⁴⁵ MSIE cell proliferation was induced by activation of SV40 tumor antigen through an interferon γ (IFN γ)-inducible H-2Kb promoter at the permissive temperature (33°C). MSIE cells can survive for 3 passages under the nonpermissive temperature (37°C) in the absence of IFN γ . MSIE cells were maintained in RPMI 1640 medium supplemented with 10% fetal bovine serum (FBS), 5 U/mL murine IFN γ , 100 U/mL penicillin and streptomycin, 5 μ g/mL insulin, 5 μ g/mL transferrin, and 5 ng/mL selenous acid at 33°C with 5% CO₂.

The AGS A human gastric adenocarcinoma cell line (CRL-1739; American Type Culture Collection, Rockville, MD) and HT-29 colorectal adenocarcinoma cell line (HTB-38; American Type Culture Collection) were grown in Dulbecco's modified Eagle medium supplemented with 10% FBS and 100 U/mL penicillin and streptomycin at 37°C with 5% CO₂.

Cell Viability Assay

MSIE, AGS, and HT-29 cells were plated in 96-well plates (5000 cells/well) and cultured for 6–8 hours under normal culture conditions to allow cells to attach to the culture dish bottoms. Cells then were treated with 5-FU at concentrations ranging from 5 to 10 μ g/mL in the presence or absence of 2'-FL, α -lactose (Sigma-Aldrich, St. Louis, MO), or D-glucose (Sigma-Aldrich) at concentrations from 5 to 20 μ g/mL, or a cell-permeable caspase inhibitor, N-Benzyloxycarbonyl-Val-Ala-Asp(O-Me) fluoromethyl ketone (Z-VAD-FMK) at 20 μ mol/L (Promega, Madison, WI) for 24 hours. Cell viability was assessed with CellTiterH120 AqueousOne Solution Cell Proliferation Assays (Promega) according to the manufacturer's instructions. The standard curve for each cell line was generated and used to calculate the cell number in each group.

Cell-Cycle Assessment

MSIE and HT-29 cells were treated with 5-FU (10 μ g/mL) in the presence or absence of 2'-FL (5–20 μ g/mL) under normal culture conditions for 24 hours. The cell cycle was assessed with a Click Plus EdU 488 Flow Kit (C10632; Life Technologies Corporation, Carlsbad, CA), according to

the manufacturer's instructions. Briefly, cells were labeled with EdU and dissociated by using accutase. The cells were fixed and permeabilized, then stained with an anti-EdU antibody and propidium iodide. The cell-cycle distribution was analyzed through multicolor flow cytometry with a BD LSRII system (BD Biosciences, Franklin Lakes, NJ).

Apoptosis Assay

MSIE cells were treated with 5-FU (10 μ g/mL) in the presence or absence of 2'-FL (5–20 μ g/mL) in RPMI 1640 medium containing 1% FBS and 100 U/mL penicillin and streptomycin at 37°C for 24 hours. Attached cells were dissociated with accutase. Apoptosis was detected with a fluorescein isothiocyanate (FITC) Annexin V Apoptosis Detection Kit I (BD Biosciences) according to the manufacturer's instructions. Cells were analyzed through multicolor flow cytometry with a BD LSRII system (BD Biosciences) to determine the percentage of cells at the early apoptotic stage (FITC-Annexin-positive cells).

Cellular Lysate Collection and Western Blot Analysis

MSIE cells were cultured in RPMI 1640 medium containing 1% FBS and 100 U/mL penicillin and streptomycin, and AGS cells were cultured in Dulbecco's modified Eagle medium containing 1% FBS and 100 U/mL penicillin and streptomycin at 37°C for 24 hours. The cells were treated with 5-FU (10 μ g/mL) for 6 hours in the presence or absence of 2'-FL (5–20 μ g/mL) for 6 hours. Cells were solubilized in cell lysis buffer (Sigma-Aldrich) containing protease and phosphatase inhibitor mixture (Sigma-Aldrich). Protein concentrations of lysates were determined with a bicinchoninic acid (BCA) protein assay kit (Pierce Thermo Scientific, Waltham, MA). The lysates were mixed with Laemmli sample buffer, and equal amounts of protein were loaded for sodium dodecyl sulfate–polyacrylamide gel electrophoresis. Western blot analysis was performed with rabbit anti-cleavage caspase 3 (9661; Cell Signaling Technology, Danvers, MA) and mouse anti- β -actin (A2228; Sigma-Aldrich) antibodies. The band density was measured using the ImageJ processing program (National Institutes of Health, Bethesda, MD). The relative density of the cleavage caspase 3 band was calculated by comparing it with the β -actin band from the same sample. The density fold change was calculated by comparison of the relative density of the band in the 5-FU and 2'-FL co-treatment groups with that in the 5-FU-treated group (which was set as 1).

Mice and Treatment

All animal experiments were performed according to protocols approved by the Institutional Animal Care and Use Committee at Vanderbilt University Medical Center. Wild-type C57BL/6J mice (000664; Jackson Laboratory, Bar Harbor, ME) received 2'-FL supplementation in drinking water (1 mg/mL) 4 days before (pretreatment) or concurrently with the induction of intestinal mucositis by intraperitoneal injection of 5-FU (Sigma-Aldrich) in PBS (250 mg/kg body weight). Mice treated with PBS were used as

negative controls. Mice were killed 1 day or 4 days after 5-FU injection. The treatment plans are shown in [Figure 5A](#) and [Figure 6A](#). Body weights were recorded. The percentage change compared with

the body weight before 5-FU injection was used to evaluate the loss of body weight.

Enteroid Culture and Treatment

Villi from the ileum of wild-type C57BL/6 mice were prepared for culture of enteroids, as described before.⁴⁶ Enteroids were cultured in Matrigel (354248; Corning Incorporated, Corning, NY) and overlaid with IntestiCult Organoid Growth Medium (06005; STEMCELL Technologies, Vancouver, Canada) for 4–5 days until budding. Enteroids were treated with 5-FU (10 $\mu\text{g}/\text{mL}$) in medium for 6 hours with and without 2'-FL (20 $\mu\text{g}/\text{mL}$ in medium) treatment, including 24-hour pretreatment and 6-hour co-treatment with 5-FU. Enteroids were fixed in 4% paraformaldehyde overnight at 4°C for immunostaining.

Evaluation of Villus Length and Intestinal Mucositis

The ileum was paraffin-embedded and processed. Tissue sections of the ileum were stained with H&E. Slides were scanned with a Leica SCN400 Slide Scanner (Leica Microsystems, Wetzlar, Germany). The villus length was analyzed in the associated software package with complex algorithms. At least 3 segments of ileum (1-cm long) were chosen for each mouse. At least 100 villi in each 1-cm long segment were measured. The average villus length was calculated for each mouse.

Samples were examined by a pathologist blinded to treatment conditions for assessing inflammation. The scoring system used to assess 5-FU-induced mucositis was modified from a previous scoring system,²⁷ including villous atrophy, epithelial injury, acute inflammation, chronic inflammation, and depth of inflammation, on a scale of 0–3, thus yielding an additive score between 0 (no mucositis) and 15 (maximal mucositis).

Quantification of MPO in Small Intestinal Tissues by ELISA

Small intestinal tissues were weighed and homogenized in PBS with a TissueLyser (Qiagen, Germantown, MD) (0.2 mg tissues/mL PBS) and sonicated. The tissue suspensions were centrifuged. The level of MPO in supernatants was measured using a Myeloperoxidase Mouse ELISA Kit (Invitrogen/Thermo Fisher Scientific, Waltham, MA), according to the manufacturer's instructions. Recombinant mouse MPO was used to generate a standard concentration curve. The MPO concentration was representative as nanograms of MPO per gram of tissue.

Immunostaining

Paraffin-embedded tissue sections were deparaffinized, and this was followed by antigen unmasking by incubation in Diva Decloaker (Biocare Medical, Concord, CA) in a

pressure cooker for 20 minutes. Tissue sections were stained with rabbit anti-Ki67 monoclonal antibody (Biocare Medical) overnight at 4°C or rabbit anti-MUC2 antibody (Santa Cruz Biotechnology, Dallas, TX) for 48 hours at 4°C, followed by a 1-hour incubation with goat anti-rabbit polymer-horseradish-peroxidase secondary antibody (Biocare Medical) at room temperature. The sections were developed with ImmPACT 3,3'-diaminobenzidine tetra hydrochloride substrate (Vector Laboratories, Inc, Burlingame, CA) and counterstained with hematoxylin. Apoptosis in tissue sections was detected with an ApopTag In Situ Oligo Ligation Kit (MilliporeSigma, Burlington, MA), according to the manufacturer's instructions. Sections were counterstained with methyl green. Bright-field sections were scanned using the Leica SCN400 Slide Scanner. At least 3 segments of the ileum (1-cm long) were chosen from each mouse. The number of positive Ki67, MUC2, and terminal deoxynucleotidyl transferase-mediated deoxyuridine triphosphate nick-end labeling cells were counted in at least 100 villi in each 1-cm long segment. The ZO-1 staining was performed by incubating tissue sections with a rabbit anti-mouse ZO-1 antibody (61-7300; Invitrogen Life Technologies) overnight at 4°C and a FITC-labeled goat anti-rabbit IgG antibody (111-095-003; Jackson ImmunoResearch, West Grove, PA) at room temperature for 1 hour. Fluorescent sections were scanned using the Leica Apero Versa 200 platform.

Fixed enteroids were permeabilized for cleavage caspase 3 and E-cadherin double staining. Enteroids were incubated with a rabbit anti-cleavage caspase 3 antibody (9661; Cell Signaling Technology) overnight, followed by a mouse anti-E-cadherin antibody (610181; BD Biosciences) for 1 hour at 4°C. Then, sections were incubated sequentially with FITC-labeled anti-rabbit IgG (111-095-003; Jackson ImmunoResearch) and Cy3-labeled anti-mouse IgG (115-165-003; Jackson ImmunoResearch) secondary antibodies for 1 hour for each antibody at room temperature. Sections were mounted using Mounting Medium containing 4',6-diamidino-2-phenylindole (P36931; Invitrogen/Thermo Fisher Scientific) for nuclear counterstaining. Sections were observed using the Nikon (Tokyo, Japan) spinning disk confocal platform and images were recorded using the Andor DU-897 EMCCD camera.

Reverse-Transcription PCR Assay

Ileal tissues were homogenized with a TissueLyser (Qiagen) for RNA isolation with a RNeasy Mini Kit (Qiagen). RNA was treated with RNase-free DNase (Qiagen). Reverse transcription was performed with a high-capacity complementary DNA reverse-transcription Kit (Applied Biosystems, Foster City, CA). Reverse-transcription PCR was performed with the 7300 Reverse-Transcription PCR System (Applied Biosystems) and primers for mouse TNF (Mm00443259; Applied Biosystems) and mouse glyceraldehyde-3-phosphate dehydrogenase (4352339; Applied Biosystems). The relative abundance of mouse glyceraldehyde-3-phosphate dehydrogenase mRNA was used to normalize levels of the mRNAs of interest.

Analysis of the Gut Microbiota by High-Throughput Genomic Sequencing

Mouse feces were collected in a Stool Nucleic Acid Collection and Preservation Tube (45630; Norgen Biotek Corporation, Thorold, Ontario, Canada). Fecal genomic DNA was extracted using the PowerSoil Pro kit (47016; Qiagen). The bacterial abundance in feces was examined using high-throughput genomic sequencing by One Codex (San Francisco, CA). The library was constructed using the Kapa HyperPlus kit (07962428001; Roche Sequencing and Life Science, Indianapolis, IN). Sequencing was performed using Illumina's NovaSeq 6000 platform (San Diego, CA) with a target of 4 million of 2×150 -bp reads per sample. Identification of bacterial sequences was performed using 2 reference databases, the One Codex database and a database containing more than 8000 bacterial genomes in the National Center for Biotechnology Information (NCBI) RefSeq database. The One Codex database consists of 115,000 complete bacterial genomes, including bacterial, viral, archaeal, and eukaryotic genomes (<https://app.onecodex.com/references>). The human and mouse genomes were included to screen out host reads. Three sequential steps were applied to comparing a bacterial sample against these reference databases: k-mer-based taxonomic classification algorithm through a web-based data platform,^{47,48} artifact filtering, and species-level abundance estimation. The relative abundance of each bacterial species was estimated through the assessment of the depth and coverage of sequencing across every available reference genome. The scikit bio package (v0.5.6; <http://scikit-bio.org/docs/0.5.6/index>) was used to calculate the α - and β -diversity metrics.

Statistical Analysis

All data are presented as means \pm SD. Statistical significance was determined using 1-way analysis of variance, followed by the Tukey multiple comparisons test or unpaired *t* test for comparing data from 2 samples using GraphPad Prism 9.0 (GraphPad Software, Inc, San Diego, CA). R^2 and *P* values for comparing weighted UniFrac β -diversity between 2 groups were examined using the permutational multivariate analysis of variance test implemented in the R package vegan.⁴⁹ A *P* value less than .05 was defined as statistically significant.

Results reported from in vitro studies represent data from at least 3 independent experiments. Data from all mice in this study were included in the analysis.

All authors had access to the study data and reviewed and approved the final manuscript.

References

- Ballard O, Morrow AL. Human milk composition: nutrients and bioactive factors. *Pediatr Clin North Am* 2013; 60:49–74.
- Victora CG, Bahl R, Barros AJ, Franca GV, Horton S, Krasevec J, Murch S, Sankar MJ, Walker N, Rollins NC. Lancet Breastfeeding Series Group. Breastfeeding in the 21st century: epidemiology, mechanisms, and lifelong effect. *Lancet* 2016;387:475–490.
- Bode L. Human milk oligosaccharides: every baby needs a sugar mama. *Glycobiology* 2012;22:1147–1162.
- Bode L, Jantscher-Krenn E. Structure-function relationships of human milk oligosaccharides. *Adv Nutr* 2012; 3:383S–391S.
- Zeuner B, Teze D, Muschiol J, Meyer AS. Synthesis of human milk oligosaccharides: protein engineering strategies for improved enzymatic transglycosylation. *Molecules* 2019;24:2033.
- Blank D, Dotz V, Geyer R, Kunz C. Human milk oligosaccharides and Lewis blood group: individual high-throughput sample profiling to enhance conclusions from functional studies. *Adv Nutr* 2012;3:440S–449S.
- Lis-Kuberka J, Orczyk-Pawilowicz M. Sialylated oligosaccharides and glycoconjugates of human milk. The impact on infant and newborn protection, development and well-being. *Nutrients* 2019;11:306.
- Plaza-Diaz J, Fontana L, Gil A. Human milk oligosaccharides and immune system development. *Nutrients* 2018;10:1038.
- Triantis V, Bode L, van Neerven RJJ. Immunological effects of human Mmlk oligosaccharides. *Front Pediatr* 2018;6:190.
- Chambers SA, Townsend SD. Like mother, like microbe: human milk oligosaccharide mediated microbiome symbiosis. *Biochem Soc Trans* 2020;48:1139–1151.
- Marcobal A, Sonnenburg JL. Human milk oligosaccharide consumption by intestinal microbiota. *Clin Microbiol Infect* 2012;18(Suppl 4):12–15.
- Craft KM, Townsend SD. Mother knows best: deciphering the antibacterial properties of human milk oligosaccharides. *Acc Chem Res* 2019;52:760–768.
- Thurl S, Munzert M, Boehm G, Matthews C, Stahl B. Systematic review of the concentrations of oligosaccharides in human milk. *Nutr Rev* 2017;75:920–933.
- Lagstrom H, Rautava S, Ollila H, Kaljonen A, Turta O, Makela J, Yonemitsu C, Gupta J, Bode L. Associations between human milk oligosaccharides and growth in infancy and early childhood. *Am J Clin Nutr* 2020;111:769–778.
- Yu ZT, Chen C, Kling DE, Liu B, McCoy JM, Merighi M, Heidtman M, Newburg DS. The principal fucosylated oligosaccharides of human milk exhibit prebiotic properties on cultured infant microbiota. *Glycobiology* 2013; 23:169–177.
- Elison E, Vigsnaes LK, Rindom Krogsgaard L, Rasmussen J, Sorensen N, McConnell B, Hennem T, Sommer MO, Bytzer P. Oral supplementation of healthy adults with 2'-O-fucosyllactose and lacto-N-neotetraose is well tolerated and shifts the intestinal microbiota. *Br J Nutr* 2016;116:1356–1368.
- Grabinger T, Glaus Garzon JF, Hausmann M, Geirnaert A, Lacroix C, Hennem T. Alleviation of intestinal inflammation by oral supplementation with 2-fucosyllactose in mice. *Front Microbiol* 2019;10:1385.
- He Y, Liu S, Kling DE, Leone S, Lawlor NT, Huang Y, Feinberg SB, Hill DR, Newburg DS. The human milk oligosaccharide 2'-fucosyllactose modulates CD14

- expression in human enterocytes, thereby attenuating LPS-induced inflammation. *Gut* 2016;65:33–46.
19. Sonis ST. The pathobiology of mucositis. *Nat Rev Cancer* 2004;4:277–284.
 20. Kwon Y. Mechanism-based management for mucositis: option for treating side effects without compromising the efficacy of cancer therapy. *Onco Targets Ther* 2016; 9:2007–2016.
 21. Cinausero M, Aprile G, Ermacora P, Basile D, Vitale MG, Fanotto V, Parisi G, Calvetti L, Sonis ST. New frontiers in the pathobiology and treatment of cancer regimen-related mucosal injury. *Front Pharmacol* 2017;8:354.
 22. Longley DB, Harkin DP, Johnston PG. 5-fluorouracil: mechanisms of action and clinical strategies. *Nat Rev Cancer* 2003;3:330–338.
 23. Miura K, Kinouchi M, Ishida K, Fujibuchi W, Naitoh T, Ogawa H, Ando T, Yazaki N, Watanabe K, Haneda S, Shibata C, Sasaki I. 5-FU metabolism in cancer and orally-administrable 5-fu drugs. *Cancers (Basel)* 2010; 2:1717–1730.
 24. Allaire JM, Crowley SM, Law HT, Chang SY, Ko HJ, Vallance BA. The intestinal epithelium: central coordinator of mucosal immunity. *Trends Immunol* 2018; 39:677–696.
 25. Agoston K, Hederos MJ, Bajza I, Dekany G. Kilogram scale chemical synthesis of 2'-fucosyllactose. *Carbohydr Res* 2019;476:71–77.
 26. De Angelis PM, Svendsrud DH, Kravik KL, Stokke T. Cellular response to 5-fluorouracil (5-FU) in 5-FU-resistant colon cancer cell lines during treatment and recovery. *Mol Cancer* 2006;5:20.
 27. Soares PM, Mota JM, Gomes AS, Oliveira RB, Assreuy AM, Brito GA, Santos AA, Ribeiro RA, Souza MH. Gastrointestinal dysmotility in 5-fluorouracil-induced intestinal mucositis outlasts inflammatory process resolution. *Cancer Chemother Pharmacol* 2008; 63:91–98.
 28. Johansson ME, Sjoval H, Hansson GC. The gastrointestinal mucus system in health and disease. *Nat Rev Gastroenterol Hepatol* 2013;10:352–361.
 29. Kim YS, Ho SB. Intestinal goblet cells and mucins in health and disease: recent insights and progress. *Curr Gastroenterol Rep* 2010;12:319–330.
 30. Stringer AM, Gibson RJ, Logan RM, Bowen JM, Yeoh AS, Hamilton J, Keefe DM. Gastrointestinal microflora and mucins may play a critical role in the development of 5-fluorouracil-induced gastrointestinal mucositis. *Exp Biol Med (Maywood)* 2009;234:430–441.
 31. Kuo WT, Zuo L, Odenwald MA, Madha S, Singh G, Gurniak CB, Abraham C, Turner JR. The tight junction protein ZO-1 is dispensable for barrier function but critical for effective mucosal repair. *Gastroenterology* 2021, Epub ahead of print.
 32. Montassier E, Gastinne T, Vangay P, Al-Ghalith GA, Bruley des Varannes S, Massart S, Moreau P, Potel G, de La Cochetiere MF, Batard E, Knights D. Chemotherapy-driven dysbiosis in the intestinal microbiome. *Aliment Pharmacol Ther* 2015;42:515–528.
 33. Stringer AM. Interaction between host cells and microbes in chemotherapy-induced mucositis. *Nutrients* 2013;5:1488–1499.
 34. Kuiken NS, Rings EH, Tissing WJ. Risk analysis, diagnosis and management of gastrointestinal mucositis in pediatric cancer patients. *Crit Rev Oncol Hematol* 2015; 94:87–97.
 35. He Y, Liu S, Leone S, Newburg DS. Human colostrum oligosaccharides modulate major immunologic pathways of immature human intestine. *Mucosal Immunol* 2014; 7:1326–1339.
 36. Holscher HD, Davis SR, Tappenden KA. Human milk oligosaccharides influence maturation of human intestinal Caco-2Bbe and HT-29 cell lines. *J Nutr* 2014;144:586–591.
 37. Cheng L, Kong C, Wang W, Groeneveld A, Nauta A, Groves MR, Kiewiet MBG, de Vos P. The human milk oligosaccharides 3-FL, lacto-N-neotetraose, and LDFT attenuate tumor necrosis factor-alpha induced inflammation in fetal intestinal epithelial cells in vitro through shedding or interacting with tumor necrosis factor receptor 1. *Mol Nutr Food Res* 2021;65:e2000425.
 38. Moremen KW, Tiemeyer M, Nairn AV. Vertebrate protein glycosylation: diversity, synthesis and function. *Nat Rev Mol Cell Biol* 2012;13:448–462.
 39. Kuntz S, Rudloff S, Kunz C. Oligosaccharides from human milk influence growth-related characteristics of intestinally transformed and non-transformed intestinal cells. *Br J Nutr* 2008;99:462–471.
 40. Thaiss CA, Zmora N, Levy M, Elinav E. The microbiome and innate immunity. *Nature* 2016;535(7610):65–74.
 41. Yeung CY, Chiang Chiau JS, Cheng ML, Chan WT, Chang SW, Chang YH, Jiang CB, Lee HC. Modulations of probiotics on gut microbiota in a 5-fluorouracil-induced mouse model of mucositis. *J Gastroenterol Hepatol* 2020;35:806–814.
 42. Wardill HR, van der Aa SAR, da Silva Ferreira AR, Havinga R, Tissing WJE, Harmsen HJM. Antibiotic-induced disruption of the microbiome exacerbates chemotherapy-induced diarrhoea and can be mitigated with autologous faecal microbiota transplantation. *Eur J Cancer* 2021;153:27–39.
 43. Laharie D, Asencio C, Asselineau J, Bulois P, Bourreille A, Moreau J, Bonjean P, Lamarque D, Pariente A, Soule JC, Charachon A, Coffin B, Perez P, Megraud F, Zerbib F. Association between enterohepatic *Helicobacter* species and Crohn's disease: a prospective cross-sectional study. *Aliment Pharmacol Ther* 2009;30:283–293.
 44. Zhou G, Liu X, Su D, Li L, Xiao M, Wang PG. Large scale enzymatic synthesis of oligosaccharides and a novel purification process. *Bioorg Med Chem Lett* 2011; 21:311–314.
 45. Whitehead RH, VanEeden PE, Noble MD, Ataliotis P, Jat PS. Establishment of conditionally immortalized epithelial cell lines from both colon and small intestine of adult *H-2Kb-tsA58* transgenic mice. *Proc Natl Acad Sci U S A* 1993;90:587–591.
 46. Wang Y, Liu L, Moore DJ, Shen X, Peek RM, Acra SA, Li H, Ren X, Polk DB, Yan F. An LGG-derived protein promotes IgA production through upregulation of APRIL

expression in intestinal epithelial cells. *Mucosal Immunol* 2017;10:373–384.

47. Ames SK, Hysom DA, Gardner SN, Lloyd GS, Gokhale MB, Allen JE. Scalable metagenomic taxonomy classification using a reference genome database. *Bioinformatics* 2013;29:2253–2260.
48. Wood DE, Salzberg SL. Kraken: ultrafast metagenomic sequence classification using exact alignments. *Genome Biol* 2014;15:R46.
49. Oksanen J, Blanchet FG, Kindt R, et al. Package 'vegan'. *Community ecology package, version* 2013;2(9):1–295.

Received May 13, 2021. Accepted September 22, 2021.

Correspondence

Address correspondence to: Fang Yan, MD, PhD, Department of Pediatrics, Vanderbilt University Medical Center, 2215 Garland Avenue, MRB IV, Room 1035, Nashville, Tennessee 37232-0696. e-mail: fang.yan@vumc.org; fax: (615) 343-5323.

Acknowledgments

The authors thank the Digital Histology Shared Resource at Vanderbilt University Medical Center (www.mc.vanderbilt.edu/dhsr) for whole slide imaging.

CRedit Authorship Contributions

Gang Zhao, PhD (Conceptualization: Equal; Data curation: Equal; Formal analysis: Equal; Writing – original draft: Supporting)
 Jessica Williams, BS (Data curation: Equal; Formal analysis: Supporting)
 M. Kay Washington, MD, PhD (Data curation: Supporting; Formal analysis: Supporting)
 Yaohua Yang, PhD (Formal analysis: Equal; Methodology: Equal)
 Jirong Long, PhD (Formal analysis: Supporting; Methodology: Supporting)
 Steven D Townsend, PhD (Conceptualization: Supporting; Data curation: Supporting; Formal analysis: Supporting; Funding acquisition: Supporting; Writing – original draft: Supporting; Writing – review & editing: Supporting)
 Fang Yan, MD, PhD (Conceptualization: Lead; Data curation: Equal; Formal analysis: Lead; Funding acquisition: Lead; Methodology: Lead; Project administration: Lead; Supervision: Lead; Writing – original draft: Lead; Writing – review & editing: Lead)

Conflicts of interest

The authors disclose no conflicts.

Funding

This work was supported by National Institutes of Health grant R01DK081134 and a Crohn's and Colitis Foundation Senior Research Award (F.Y.); National Institutes of Health grant R35GM133602, a Dean's Faculty Fellowship from the College of Arts and Science at Vanderbilt University, a Camille Dreyfus Teacher Scholar award, and a fellowship from the Alfred P. Sloan Foundation (S.D.T.); and by core services performed through Vanderbilt University Medical Center's Digestive Disease Research Center, supported by National Institutes of Health grant P30DK058404.